



Published in final edited form as:

Cancer Res. 2012 February 1; 72(3): 716–725. doi:10.1158/0008-5472.CAN-10-2873.

Anti-tumor and anti-angiogenic effects of metronomic dosing of BH3-mimetics

Atsushi Imai¹, Benjamin D. Zeitlin^{1,6}, Fernanda Visioli¹, Zhihong Dong¹, Zhaocheng Zhang¹, Sudha Krishnamurthy¹, Emily Light², Frank Worden³, Shaomeng Wang³, and Jacques E. Nör^{1,4,5}

¹Angiogenesis Research Laboratory, Department of Restorative Sciences, University of Michigan School of Dentistry, Ann Arbor, Michigan

²Biostatistic Unit, University of Michigan Comprehensive Cancer Center, San Francisco, California

³Department of Internal Medicine, University of Michigan School of Medicine, San Francisco, California

⁴Department of Biomedical Engineering, University of Michigan College of Engineering, San Francisco, California

⁵Department of Otolaryngology, University of Michigan School of Medicine, San Francisco, California

⁶Department of Physiological Sciences, University of the Pacific, San Francisco, California

Abstract

Recent studies have shown that Bcl-2 functions as a pro-angiogenic signaling molecule in addition to its well-known effect as an inhibitor of apoptosis. The discovery of AT101, a BH3-mimetic drug that is effective and well tolerated when administered orally, suggested the possibility of using a molecularly targeted drug in a metronomic regimen. Here, we generated xenograft squamous cell carcinomas (SCC) with humanized vasculature in immunodeficient mice. Mice received taxotere in combination with either daily 10 mg/kg AT101 (metronomic regimen) or weekly 70 mg/kg AT101 (bolus regimen). The effect of single drug AT101 on angiogenesis, and combination AT101/taxotere on the survival of endothelial cells and SCC cells, were also evaluated *in vitro*. Metronomic AT101 increased mouse survival ($p=0.02$), decreased tumor mitotic index ($p=0.0009$), and decreased tumor microvessel density ($p=0.0052$), as compared to bolus delivery of AT101. Notably, the substantial potentiation of the anti-tumor effect observed in the metronomic AT101 group was achieved using the same amount of drug and without significant changes in systemic toxicities. *In vitro*, combination of AT101 and taxotere showed additive toxicity for endothelial cells and synergistic or additive toxicity for tumor cells (SCC). Interestingly, low-dose (sub-apoptotic) concentrations of AT101 potently inhibited the angiogenic potential of endothelial cells. Taken together, these data unveiled the benefit of metronomic delivery of a molecularly targeted drug, and suggested that patients with squamous cell carcinomas might benefit from continuous administration of low dose BH3-mimetic drugs.

Corresponding author Jacques E. Nör DDS, PhD, Angiogenesis Research Laboratory, University of Michigan, 1011 N. University Rm.2309, Ann Arbor, MI 48109-1078, Telephone: (734)936-9300, jenor@umich.edu.

Disclosure of Potential Conflicts of Interest: Shaomeng Wang owns stocks, stock options and serves as a consultant for Ascenta Therapeutics that has licensed technologies related to AT101 from the University of Michigan.

Keywords

Developmental therapeutics; targeted therapy; angiogenesis; Bcl-2; squamous cell carcinoma

Introduction

Induction chemotherapy with taxanes, platinum-based compounds, and 5-fluorouracil is beneficial for head and neck cancer patients (1, 2), but the prolonged use of chemotherapeutic drugs is limited by their toxicity and by the development of resistance. The combined use of molecularly targeted agents with conventional therapies has been proposed more recently for management of patients with locally advanced head and neck squamous cell carcinomas (HNSCC) (3). These types of combination therapies have shown promising results, but the survival of head and neck cancer patients has not changed dramatically (4). Improvements in the survival of these patients require mechanism-based therapeutic strategies that maximize the anti-tumor effect of drugs while limiting their toxicities.

Metronomic chemotherapy has been proposed as a mean to potentiate the anti-tumor effect of chemotherapeutic drugs and to overcome drug resistance (5–7). Several independent groups have demonstrated benefits of the metronomic regimen in preclinical and clinical studies (8–10). While much has been learned about the use of conventional chemotherapeutic drugs in metronomic regimen over the last 10 years, little is known about this type of regimen with molecularly targeted drugs.

A significant proportion of head and neck tumors express high levels of anti-apoptotic Bcl-2 proteins (11, 12). Indeed, high Bcl-2 expression correlates directly with resistance to therapy with cisplatin (13), and is associated with poor clinical outcomes for head and neck cancer patients (14, 15). We have shown that Bcl-2 gene expression is significantly higher (approximately 60,000-fold) in the tumor-associated endothelial cells of patients with HNSCC, as compared to endothelial cells from the normal oral mucosa (16). Collectively, these studies provide strong rationale for the investigation of the anti-tumor and anti-angiogenic effects of drugs targeted to the Bcl-2 pathway.

BH3-mimetic compounds derived from (–)-gossypol, a natural product from cotton plant (17), inhibit the survival function of Bcl-2 family members by stimulating Noxa and Puma (18). These compounds have shown anti-tumor effect as a single agent or in combination with standard chemo-radiotherapy in various tumor models (19–21), and appear to help to overcome resistance to therapy (22–24). We have shown the potent anti-angiogenic effect (25) and anti-tumor effect of a small molecule inhibitor of Bcl-2 in head and neck cancer models (26). However, we do not understand the impact of the regimen of administration of a BH3-mimetic drug (AT101) on tumor growth and angiogenesis. Here, we observed that a metronomic regimen (*i.e.* daily administration of low dose AT101) has more potent anti-tumor and anti-angiogenic effects than weekly administration without compromising the low systemic toxicity profile of the drug.

Material and Methods

Cells and reagents

Primary human dermal microvascular endothelial cells (HDMEC; Lonza, Walkersville, MD) were cultured in endothelial cell growth medium (EGM2-MV; Lonza). Oral squamous cell carcinoma (OSCC3; gift from M. Linggen, University of Chicago); UM-SCC-17B and UM-SCC-74A (gift from T. Carey, University of Michigan) were cultured in DMEM (Invitrogen),

Grand Island, NY) supplemented with 10% fetal bovine serum, 200 mmol/L L-glutamine, penicillin and streptomycin at 37°C with 5% CO₂. The identity of all tumor cell lines was confirmed by genotyping at the University of Michigan DNA sequencing core facility in May/2010. For *in vitro* studies, the small molecule inhibitor of Bcl-2 (AT101) (27) and taxotere (TXT; LC laboratories, Woburn, MA) were dissolved in DMSO. For *in vivo* studies, AT101 was resuspended in carboxymethyl cellulose and sonicated for 30 minutes, while TXT was dissolved in 5% ethanol.

SRB assay

Sulforhodamine B (SRB) cytotoxicity assays were done as described (25). Briefly, cells were seeded at 2×10^3 cells per well of 96-well plates, allowed to attach overnight, and treated with AT101 and/or taxotere for 72–96 hours. Cells were fixed with 10% trichloroacetic acid, stained with 0.4% SRB (Sigma-Aldrich, St. Louis, MO) in 1% acetic acid, and plates were read in a microplate reader at 560 nm (GENios; Tecan, Graz, Austria). Test results were normalized against initial plating density and drug-free controls. Data were obtained from triplicate wells per condition and is representative of three independent experiments.

Droplet assay

Droplets were formed by mixing HDMEC and 10% sucrose containing 0.05% puramatrix (BD Biosciences, San Jose, CA). Droplet was transferred to type I collagen (Angiotech BioMaterials, Palo Alto, CA) coated plates and covered with collagen containing 50 ng/ml rhVEGF₁₆₅ (R&D Systems, Minneapolis, MN). Treatment started as soon as sprout outgrowth was visible. Drug containing medium was changed every day in the metronomic group while in the bolus treatment group the complete dose was delivered in the first day. Data were obtained from triplicate wells per condition and is representative of three independent experiments.

SCID Mouse Model of Human Tumor Angiogenesis

Xenograft human tumors vascularized with human blood vessels were generated as described (28). Briefly, highly porous poly-(L-lactic) acid scaffolds seeded with 9×10^5 HDMEC and 1×10^5 tumor cells (OSCC3) were incubated for 30 minutes at 37°C. Male severe combined immunodeficient (SCID) mice (Charles River Laboratory, Portage, MI) were anesthetized with ketamine and xylazine, and scaffolds were implanted subcutaneously in the dorsal region of each mouse. When tumor size reached 200 mm³, mice were randomized into 4 groups: vehicle, $n=8$; taxotere, $n=7$; weekly AT101+taxotere (bolus), $n=8$; daily AT101+taxotere (metronomic), $n=8$. At termination of the experiment, mice were euthanized, tumors were retrieved, fixed overnight in 10% buffered formalin at 4°C, and processed for histology. The histopathology was assessed by a trained pathologist unaware of treatment conditions. The mitotic index was determined by counting mitotic figures in 10 high power fields (HPF) per tumor section and then averaging the number by HPF area (0.096 mm²) and expressed as the number of mitoses per square millimeter of primary tumor (29). Mice were euthanized whenever the tumor volume reached 2,000 mm³ following the University of Michigan Guidelines for Use and Care of Animals. Tumor size was calculated using the formula: volume (mm³) = $L \times W^2/2$ (L , length; W , width).

Immunohistochemistry

Paraffin embedded tissue sections were incubated in antigen retrieval solution (Dako, Carpinteria, CA) for 20 minutes at 90–95°C. Tissues were exposed to 1:500 dilution of the anti-human factor VIII antibody (NeoMarkers, Fremont, CA) overnight at 4°C, as described (28). Blood vessels were counted in 6 random fields per tumor, from 7–8 tumors per group.

Statistical Analysis

Time to failure data was analyzed using the Kaplan-Meier method and the log-rank test. Where multiple fields were measured, the average was taken for each mouse. Continuous measurements, such as tumor volume, average mitosis per mm² and average microvessel density were analyzed using nonparametric rank-based Wilcoxon tests and Kruskal-Wallis tests. The growth curve of tumor volume (mm³) was transformed by log₂ in order to improve linearity assumptions of residuals for longitudinal modeling. We refer to this transformation as log₂ tumor volume and can be interpreted as tumor doubling. A longitudinal mixed model was used to test the difference in growth patterns based on treatment group. Kaplan-Meier analysis, longitudinal analysis and Wilcoxon tests were performed using SAS v9.2 software. *In Vitro* statistical analysis was performed using ANOVA followed by Tukey's test (SigmaStat 2.0 software; SPSS, Chicago, IL). The synergism or additivity was calculated using the combinatorial index (CI), a mathematical and quantitative evaluation of a two-drug pharmacologic interaction (30). Using CalcuSyn ver. 2.0 software (Biosoft, Cambridge, UK), CI values were generated over a range of fractional cell kill levels (Fa) from 0.05 to 0.95 (5–95% cell kill). Accordingly, a synergistic effect is represented by CI<0.9; an additive effect by 0.9 < CI < 1.1; and absence of combinatorial effect CI>1.1. Statistical significance was defined as $p<0.05$, unless otherwise specified.

Results

Metronomic AT101 enhances the time to failure of xenograft head and neck tumors

To investigate the effect of metronomic (low dose, high frequency) versus bolus (high dose, low frequency) administration of a BH3-mimetic drug on tumor growth, we generated xenografts with humanized vasculature (31, 32). All experimental conditions included low dose taxotere (5 mg/kg taxotere, once a week) to mimic the most probable clinical scenario for the use of the targeted drug in combination with a conventional chemotherapeutic drug. The maximum tolerated dose (MTD) for BH3-mimetic was estimated to be around 40 mg/kg for 3 days (20) and for taxotere around 50 mg/kg weekly (33) In pilot experiments, we observed that oral administration of 105 mg/kg AT101 plus 5 mg/kg taxotere weekly caused 15–20% weight loss, and was considered to be the MTD for the combination therapies (data not shown). These studies also showed that weekly 70 mg/kg AT101 plus 5 mg/kg taxotere was well tolerated by mice (<15% weight loss).

The criterion to determine failure for the Kaplan-Meier analysis was a tumor volume of 2,000 mm³, which coincided with the indication for mouse euthanasia. These experiments were performed with an aggressive squamous cell carcinoma (OSCC3), and therefore the time to failure was as low as 13 days (vehicle control). The average time to failure was 20.8 days (vehicle, $n=8$), 24.9 days (taxotere, $n=7$), 28.9 days (weekly AT101+taxotere, $n=8$), and 37.8 days (daily AT101+taxotere, $n=8$). The distribution of time to failure was significantly different across the four groups ($p<0.0001$) (Fig. 1A). Daily AT101+taxotere mediated a significant delay in time to failure as compared to all other experimental conditions (Fig. 1A). In pairwise comparisons, survival was prolonged by daily AT101+taxotere treatment as compared to weekly AT101+taxotere ($p=0.02$), to taxotere ($p=0.0006$), or to vehicle control ($p<0.0001$). Weekly AT101+taxotere improved survival when compared to vehicle control ($p=0.03$), but had no benefit when compared to taxotere alone ($p=0.30$). Starting at day 5 of treatment and continuing thereafter, the tumor volume in mice that received daily AT101+taxotere was consistently lower than the tumor volume in mice treated with weekly AT101+taxotere (Fig. 1B). For example, at day 5 the difference between daily AT101+taxotere *versus* weekly AT101+taxotere had a $p=0.0181$. Figure 1C depicts a detailed analysis of tumor volume after 13 days of treatment, the time when we had

to begin to euthanize animals from the untreated control group. Again, tumor volume was reduced in the daily AT101+taxotere as compared to the weekly AT101+taxotere group ($p=0.0313$). Notably, we did not observe deaths attributed to drug toxicity with the regimens used here, and the average weight loss was consistently less than 15% (Fig. 1D). Moreover, no signs of toxicity were observed in vital organs including liver and lung (Supplementary Fig. S1).

Tumors treated with metronomic AT101 combined with taxotere were less aggressive and less vascularized

In general, xenografts showed tumor cells with basophile cytoplasm, increased nuclear-to-cytoplasm diameter ratio, and marked cellular pleomorphism (Fig. 2A). In contrast, the metronomic AT101+taxotere group presented a distinct pattern, with a large proportion of clear cells (Fig. 2A). The tumor cells presented clear cytoplasm and smaller nucleus with higher condensation of chromatin. In addition larger necrotic areas were observed (Fig. 2A). We observed a significant overall difference in mitotic index (Fig. 2B, KW $p=0.0007$) and tumor microvessel density (Fig. 2C, KW $p=0.0042$). Pairwise analysis revealed that the mitotic index of daily AT101+taxotere was lower than the mitotic index of each one of the other experimental conditions, as follows ($p=0.0014$, compared to vehicle; $p=0.0428$, compared to taxotere; and $p=0.0009$, compared to weekly AT101+taxotere) (Fig. 2B). We also observed that the microvessel density in the daily AT101+taxotere group was lower than in the vehicle control ($p=0.0053$), taxotere only ($p=0.0233$), and weekly AT101+taxotere ($p=0.0052$) (Fig. 2C). Moreover, qualitative assessment revealed that the daily AT101+taxotere regimen induced more tumor cell apoptosis, as compared to the other experimental conditions (Supplementary Fig. S2).

***In vitro* analyses of the cytotoxic effects of AT101 and taxotere**

The IC_{50} for AT101 was 0.80 μ M (HDMEC) and ranged from 1.50 to 2.54 μ M for head neck tumor cells (OSCC3, UM-SCC-17B, UM-SCC-74A) (Fig. 3). The IC_{50} for taxotere was 0.37 nM (HDMEC), and ranged from 0.20 to 0.53 nM for the tumor cells evaluated (Fig. 3). The IC_{25} and IC_{75} of these two drugs were also calculated in a separate set of experiments with narrower range of drug concentrations (data not shown).

To investigate whether AT101 sensitizes HDMEC and tumor cells to chemotherapy, we examined the cytotoxic effects of the IC_{25} , IC_{50} , IC_{75} concentrations for each drug by itself or in combination. Synergistic and/or additive effects were observed primarily when higher concentrations of AT101 were combined with taxotere for all cell types examined here (Fig. 4). Interestingly, the overall trends for the combinatorial index (CI) analysis were similar for endothelial cells and head and neck tumor cells (Fig. 4).

Next, we investigated the effect of treatment sequence on the cytotoxicity of these drugs in HDMEC and tumor cells. For each cell type, we either pre-treated cells with one drug for 24 hours, or started treatment together with the two drugs. The drug concentration was set at the IC_{50} , and two time periods were evaluated to factor-in the overall time of treatment on the effects observed. We observed that starting the two drugs at the same time provided the highest cytotoxic effect for all cell types evaluated here ($p<0.01$) (Fig. 5). Propidium iodide staining followed by flow cytometry was performed to observe the effects of different treatment sequence on apoptosis and cell cycle of OSCC3. The use of both drugs at the same time induced more apoptosis than any other experimental condition tested here ($p<0.05$) (Supplementary Fig. S3A). Cell cycle analysis showed that starting the treatment with AT101 and taxotere at the same time significantly increases the S-phase fraction (Supplementary Fig. S3B,C), which is consistent with the S-phase cell cycle arrest reported previously for another BH3 mimetics drug (*i.e.* TW37) (26, 34).

Effect of AT101 regimen on the angiogenic potential of endothelial cells in 3-D matrices

AT101 ((-)-gossypol) has been developed and characterized as a functional inhibitor of Bcl-2 via binding to BH3-binding domain and interference with the interaction of Bcl-2 with other BH3-containing pro-apoptotic proteins (35, 36). As expected, Bcl-2 expression was not affected by AT101 treatment (Supplementary Fig. 4), confirming previous observations (23). To evaluate the anti-angiogenic effect of AT101 *in vitro*, we created 3-D droplets of endothelial cells and plated them in collagen matrices. Endothelial cells were induced to sprout with VEGF, and 0.1×IC₅₀ (0.08 μM), IC₅₀ (0.8 μM), 10×IC₅₀ (8 μM) AT101 were used. We either administered these dosages at once (bolus), or mimicked the metronomic regimen by dividing them in 4 daily administrations. The highest concentration of AT101 eliminated capillary sprouts by 4 days in both regimens (Fig. 6). For both 0.1×IC₅₀ and IC₅₀ conditions, the daily administration of the drug led to more potent reduction in capillary sprouting than the administration of the same overall dosage at once (0.08 μM daily *versus* 0.08 μM bolus; $p < 0.001$, 0.8 μM daily *versus* 0.8 μM bolus; $p = 0.023$) (Fig. 6B). Interestingly, the lowest concentration of AT101 used here (0.08 μM AT101) induced a potent anti-angiogenic effect ($p < 0.001$), despite the fact that this concentration is sub-apoptotic (Fig. 6B). These data corroborated our previous reports that Bcl-2 functions as a pro-angiogenic signaling molecule (37), in addition to its well-known effects on the regulation of endothelial cell survival (28).

Discussion

Improvements in the survival of head and neck cancer patients will most likely come from the development and characterization of mechanism-based therapies that combine the potency of cytotoxic drugs with the specificity of molecularly targeted agents. Evidence clearly demonstrates the role of Bcl-2 in the poor outcomes of patients with head and neck cancer (38). We have also shown that Bcl-2 plays a dominant role in head and neck tumor angiogenesis and tumor growth (16, 25, 31, 39). Therefore, targeting the Bcl-2 system is appealing because it has two complimentary effects mediated by the direct induction of tumor cell apoptosis and the selective disruption of tumor blood vessels (36).

The combination of the BH3-mimetic drug AT101 with taxotere, a microtubule-binding drug with significant antitumor activity, was selected for these experiments. Although taxotere is widely used in many tumor types including head and neck cancer, strong side effects such as myelosuppression have suggested that combination therapies that allow for a reduction of its dosage are highly desirable (1, 40, 41). Likewise, although single drug therapy with BH3 mimetics partially inhibits tumor growth in some cancer models (42, 43), combination therapies tend to enhance the efficacy of the BH3 mimetics (44, 45). Notably, it has been recently reported that the combination of BH3 mimetic with taxotere inhibits tumor cell growth and affects expression of several genes involved in drug resistance, drug metabolism, DNA repair, cell cycle and oncogenes in a prostate tumor cell line (PC3) (22). Here, we observed that the combination of AT101 with taxotere augments the anti-tumor cell and anti-angiogenic effects of each one of these drugs used individually. Notably, best results were achieved with higher doses of AT101, a drug with minimal systemic cytotoxicities, combined with lower doses of taxotere. Collectively these data unveils a drug combination that is highly effective *in vivo* while showing modest systemic cytotoxic effects.

Metronomic therapy of DNA-damaging agents or microtubule inhibitors has shown more efficiency than MTD therapy in randomized phase III clinical trials (46, 47). Metronomic therapy of certain drugs induces sustained suppression of circulating endothelial progenitor cells (CEP), while MTD schedules appear to allow for rebound vessel repair responses mediated primarily by bone marrow cell recruitment (44). Here, we examined the approach

of using the metronomic regimen for the molecularly targeted drug in combination with conventional regimen for chemotherapy drug. Remarkably, combination of metronomic AT101 with taxotere showed potent inhibition of tumor growth, and prolongation of the survival of mice with established tumors (as compared with bolus treatment of AT101 and taxotere) despite the fact that the total amount of drug administered in both conditions was exactly the same. We believe that this difference in response was mediated by the potentiation of both the anti-angiogenic and the tumor cell effect of AT101 when used in a metronomic regimen.

It is well known that vessel rebound rapidly occurs during the breaks in treatment (48). We postulate that by keeping constant the anti-angiogenic pressure, achieved even when very low concentrations of BH3-mimetic are used (25, 37), one does not allow for the vascular rebound and therefore the overall anti-tumor growth effect is potentiated. This hypothesis is currently under investigation in our laboratory. In addition, based on our results we speculate that low dose BH3-mimetic prevents the development of resistance of tumor cells to therapy, by interfering with the pro-survival effect of Bcl-2 family proteins. A closer look at the histopathology of tumors treated with metronomic AT101 combined with taxotere supports this hypothesis. We observed that this treatment regimen results in lower mitotic index as compared to all other treatment groups of this study. Notably, recent studies showed that the mitotic index is a potent indicator of patient survival with melanoma or breast carcinoma (49, 50). Moreover, in the metronomic AT101 group the tumor cells displayed a clear cytoplasm, suggesting glycogen accumulation compatible with chronic hypoxia and glucose deprivation. This might be related to the fact that this treatment regimen resulted in lower microvessel density.

In summary, we showed that metronomic administration of the BH3-mimetic drug AT101 in combination with low dose taxotere improves the survival of mice bearing head and neck squamous cell carcinoma xenografts. These results were correlated with lower mitotic index and tumor microvessel density. Notably, we observed that sub-apoptotic concentrations of AT101 potentially inhibited the angiogenic potential of endothelial cells. The fact that AT101 can be administered orally raises the possibility that patients could take low doses of this drug in both therapeutic as well as chemopreventive regimen. Collectively, this work unveils the anti-tumor potential of metronomic administration of a molecularly targeted drug.

Supplementary Material

Refer to Web version on PubMed Central for supplementary material.

Acknowledgments

We thank Chris Strayhorn for assistance with the histology and Naoki Ashimori for valuable suggestions.

Grant support: Grant P50-CA97248 (University of Michigan Head & Neck SPORE) from the NIH/NCI (SW, JEN) and grant U19-CA113317 (SW) from the NIH/NCI; and grants R01-DE14601, R01-DE15948, R01-DE16586, and R21-DE19279 from the NIH/NIDCR (JEN)

References

1. Posner MR, Hershock DM, Blajman CR, Mickiewicz E, Winkquist E, Gorbounova V, et al. Cisplatin and fluorouracil alone or with docetaxel in head and neck cancer. *N Engl J Med.* 2007; 357:1705–1715. [PubMed: 17960013]
2. Vermorken JB, Remenar E, van Herpen C, Gorlia T, Mesia R, Degardin M, et al. Cisplatin, fluorouracil, and docetaxel in unresectable head and neck cancer. *N Engl J Med.* 2007; 357:1695–1704. [PubMed: 17960012]

3. Langer CJ. Targeted therapy in head and neck cancer: State of the art 2007 and review of clinical applications. *Cancer*. 2008; 112:2635–2645. [PubMed: 18442098]
4. Jemal A, Siegel R, Ward E, Murray T, Xu J, Thun MJ. Cancer statistics, 2007. *CA Cancer J Clin*. 2007; 57:43–66. [PubMed: 17237035]
5. Klement G, Baruchel S, Rak J, Man S, Clark K, Hicklin DJ, et al. Continuous low-dose therapy with vinblastine and VEGF receptor-2 antibody induces sustained tumor regression without overt toxicity. *J Clin Invest*. 2000; 105:R15–R24. [PubMed: 10772661]
6. Hanahan D, Bergers G, Bergsland E. Less is more, regularly: Metronomic dosing of cytotoxic drugs can target tumor angiogenesis in mice. *J Clin Invest*. 2000; 105:1045–1047. [PubMed: 10772648]
7. Kerbel RS, Kamen BA. The anti-angiogenic basis of metronomic chemotherapy. *Nat Rev Cancer*. 2004; 4:423–436. [PubMed: 15170445]
8. Browder T, Butterfield CE, Kraling BM, Shi B, Marshall B, O'Reilly MS, et al. Antiangiogenic scheduling of chemotherapy improves efficacy against experimental drug-resistant cancer. *Cancer Res*. 2000; 60:1878–1886. [PubMed: 10766175]
9. Bello L, Carrabba G, Giussani C, Lucini V, Cerutti F, Scaglione F, et al. Low-dose chemotherapy combined with an antiangiogenic drug reduces human glioma growth *in vivo*. *Cancer Res*. 2001; 61:7501–7506. [PubMed: 11606386]
10. Pietras K, Hanahan D. A multitargeted, metronomic, and maximum-tolerated dose "chemo-switch" regimen is antiangiogenic, producing objective responses and survival benefit in a mouse model of cancer. *J Clin Oncol*. 2005; 23:939–952. [PubMed: 15557593]
11. Wang S, Yang D, Lippman ME. Targeting bcl-2 and bcl-XL with nonpeptidic small-molecule antagonists. *Semin Oncol*. 2003; 30:133–142. [PubMed: 14613034]
12. Danial NN, Korsmeyer SJ. Cell death: Critical control points. *Cell*. 2004; 116:205–219. [PubMed: 14744432]
13. Andrews GA, Xi S, Pomerantz RG, Lin CJ, Gooding WE, Wentzel AL, et al. Mutation of p53 in head and neck squamous cell carcinoma correlates with bcl-2 expression and increased susceptibility to cisplatin-induced apoptosis. *Head Neck*. 2004; 26:870–877. [PubMed: 15390206]
14. Xie X, Clausen OP, De Angelis P, Boysen M. The prognostic value of spontaneous apoptosis, bax, bcl-2, and p53 in oral squamous cell carcinoma of the tongue. *Cancer*. 1999; 86:913–920. [PubMed: 10491515]
15. Yu Y, Dong W, Li X, Yu E, Zhou X, Li S. Significance of c-myc and bcl-2 protein expression in nasopharyngeal carcinoma. *Arch Otolaryngol Head Neck Surg*. 2003; 129:1322–1326. [PubMed: 14676159]
16. Kaneko T, Zhang Z, Mantellini MG, Karl E, Zeitlin B, Verhaegen M, et al. Bcl-2 orchestrates a cross-talk between endothelial and tumor cells that promotes tumor growth. *Cancer Res*. 2007; 67:9685–9693. [PubMed: 17942898]
17. Adams R, Geissman TA, Edwards JD. Gossypol, a pigment of cottonseed. *Chem Rev*. 1960; 60:555–574. [PubMed: 13681414]
18. Meng Y, Tang W, Dai Y, Wu X, Liu M, Ji Q, et al. Natural BH3 mimetic (–)-gossypol chemosensitizes human prostate cancer via bcl-xL inhibition accompanied by increase of puma and noxa. *Mol Cancer Ther*. 2008; 7:2192–2202. [PubMed: 18645028]
19. Zeitlin BD, Spalding AC, Campos MS, Ashimori N, Dong Z, Wang S, et al. Metronomic small molecule inhibitor of Bcl-2 (TW37) is anti-angiogenic and potentiates the anti-tumor effect of ionizing radiation in oral squamous cell carcinoma xenograft. *Int J Radiat Oncol BioPhys* Forthcoming. 2010
20. Mohammad RM, Wang S, Aboukameel A, Chen B, Wu X, Chen J, et al. Preclinical studies of a nonpeptidic small-molecule inhibitor of bcl-2 and bcl-X(L) [(–)-gossypol] against diffuse large cell lymphoma. *Mol Cancer Ther*. 2005; 4:13–21. [PubMed: 15657349]
21. Wolter KG, Verhaegen M, Fernandez Y, Nikolovska-Coleska Z, Riblett M, de la Vega CM, et al. Therapeutic window for melanoma treatment provided by selective effects of the proteasome on bcl-2 proteins. *Cell Death Differ*. 2007; 14:1605–1616. [PubMed: 17541428]
22. Cengiz E, Karaca B, Kucukzeybek Y, Gorumlu G, Gul MK, Erten C, et al. Overcoming drug resistance in hormone- and drug-refractory prostate cancer cell line, PC-3 by docetaxel and gossypol combination. *Mol Biol Rep*. 2009; 37:1269–1277. [PubMed: 19288219]

23. Oliver CL, Miranda MB, Shangary S, Land S, Wang S, Johnson DE. (–)-Gossypol acts directly on the mitochondria to overcome bcl-2- and bcl-X(L)-mediated apoptosis resistance. *Mol Cancer Ther.* 2005; 4:23–31. [PubMed: 15657350]
24. Bauer JA, Trask DK, Kumar B, Los G, Castro J, Lee JS, et al. Reversal of cisplatin resistance with a BH3 mimetic, (–)-gossypol, in head and neck cancer cells: Role of wild-type p53 and bcl-xL. *Mol Cancer Ther.* 2005; 4:1096–1104. [PubMed: 16020667]
25. Zeitlin BD, Joo E, Dong Z, Warner K, Wang G, Nikolovska-Coleska Z, et al. Antiangiogenic effect of TW37, a small-molecule inhibitor of bcl-2. *Cancer Res.* 2006; 66:8698–8706. [PubMed: 16951185]
26. Ashimori N, Zeitlin BD, Zhang Z, Warner K, Turkienicz IM, Spalding AC, et al. TW-37, a small-molecule inhibitor of bcl-2, mediates S-phase cell cycle arrest and suppresses head and neck tumor angiogenesis. *Mol Cancer Ther.* 2009; 8:893–903. [PubMed: 19372562]
27. ClinicalTrials.gov [Internet]. [cited 2006 Feb 3] A Service of the U.S. National Institute of Health. Safety and Efficacy Study of AT-101 in Combination With Docetaxel and Prednisone in Men With Hormone Refractory Prostate Cancer; The reference for the clinical trials with AT101. p. c2005-c2010.updated 2010 Feb 2; Available from: <http://clinicaltrials.gov/ct2/show/NCT00286793>
28. Nör JE, Christensen J, Mooney DJ, Polverini PJ. Vascular endothelial growth factor (VEGF)-mediated angiogenesis is associated with enhanced endothelial cell survival and induction of bcl-2 expression. *Am J Pathol.* 1999; 154:375–384. [PubMed: 10027396]
29. Balch CM, Gershenwald JE, Soong SJ, Thompson JF, Atkins MB, Byrd DR, et al. Final version of 2009 AJCC melanoma staging and classification. *J Clin Oncol.* 2009; 27:6199–6206. [PubMed: 19917835]
30. Chou T, Talalay P. Quantitative analysis of dose-effect relationships: the combined effects of multiple drugs or enzyme inhibitors. *Adv Enzyme Regul.* 1984; 22:27–55. [PubMed: 6382953]
31. Nör JE, Christensen J, Liu J, Peters M, Mooney DJ, Strieter RM, et al. Upregulation of bcl-2 in microvascular endothelial cells enhances intratumoral angiogenesis and accelerates tumor growth. *Cancer Res.* 2001; 61:2183–2188. [PubMed: 11280784]
32. Nör JE, Peters MC, Christensen JB, Sutorik MM, Linn S, Khan MK, et al. Engineering and characterization of functional human microvessels in immunodeficient mice. *Lab Invest.* 2001; 81:453–463. [PubMed: 11304564]
33. Dykes DJ, Bissery MC, Harrison SD Jr, Waud WR. Response of human tumor xenografts in athymic nude mice to docetaxel (RP 56976, taxotere). *Invest New Drugs.* 1995; 13:1–11. [PubMed: 7499102]
34. Bartek J, Lukas C, Lukas J. Checking on DNA damage in S phase. *Nat Rev Mol Cell Biol.* 2004; 10:792–804. [PubMed: 15459660]
35. Wang G, Nilkolovska-Coleska Z, Yang CY, Wang R, Tang G, Guo J, et al. Structure-based design of potent small-molecule inhibitors of anti-apoptotic Bcl-2 proteins. *J Med Chem.* 2006; 49(21): 6139–6142. [PubMed: 17034116]
36. Zeitlin BD, Zeitlin IJ, Nör JE. Expanding circle of inhibition: Small-molecule inhibitors of bcl-2 as anticancer cell and antiangiogenic agents. *J Clin Oncol.* 2008; 26:4180–4188. [PubMed: 18757333]
37. Karl E, Warner K, Zeitlin B, Kaneko T, Wurtzel L, Jin T, et al. Bcl-2 acts in a proangiogenic signaling pathway through nuclear factor-kappaB and CXC chemokines. *Cancer Res.* 2005; 65:5063–5069. [PubMed: 15958549]
38. Trask DK, Wolf GT, Bradford CR, Fisher SG, Devaney K, Johnson M, et al. Expression of bcl-2 family proteins in advanced laryngeal squamous cell carcinoma: Correlation with response to chemotherapy and organ preservation. *Laryngoscope.* 2002; 112:638–644. [PubMed: 12150516]
39. Karl E, Zhang Z, Dong Z, Neiva KG, Soengas MS, Koch E, et al. Unidirectional crosstalk between bcl-xL and bcl-2 enhances the angiogenic phenotype of endothelial cells. *Cell Death Differ.* 2007; 14:1657–1666. [PubMed: 17572663]
40. Savarese DM, Halabi S, Hars V, Akerley WL, Taplin ME, Godley PA, et al. Phase II study of docetaxel, estramustine, and low-dose hydrocortisone in men with hormone-refractory prostate

- cancer: A final report of CALGB 9780. cancer and leukemia group B. *J Clin Oncol.* 2001; 19:2509–2516. [PubMed: 11331330]
41. Shepherd FA, Dancey J, Ramlau R, Mattson K, Gralla R, O'Rourke M, et al. Prospective randomized trial of docetaxel versus best supportive care in patients with non-small-cell lung cancer previously treated with platinum-based chemotherapy. *J Clin Oncol.* 2000; 18:2095–2103. [PubMed: 10811675]
 42. Wolter KG, Wang SJ, Henson BS, Wang S, Griffith KA, Kumar B, et al. (–)-Gossypol inhibits growth and promotes apoptosis of human head and neck squamous cell carcinoma *in vivo*. *Neoplasia.* 2006; 8:163–172. [PubMed: 16611409]
 43. Liu G, Kelly WK, Wilding G, Leopold L, Brill K, Somer B. An open-label, multicenter, phase I/II study of single-agent AT-101 in men with castrate-resistant prostate cancer. *Clin Cancer Res.* 2009; 15:3172–3176. [PubMed: 19366825]
 44. Mutsaers AJ. Metronomic chemotherapy. *Top Companion Anim Med.* 2009; 24:137–143. [PubMed: 19732732]
 45. Banerjee S, Choi M, Aboukameel A, Wang Z, Mohammad M, Chen J, et al. Preclinical studies of apogossypolone, a novel pan inhibitor of bcl-2 and mcl-1, synergistically potentiates cytotoxic effect of gemcitabine in pancreatic cancer cells. *Pancreas.* 2010; 39:323–331. [PubMed: 19823097]
 46. Correale P, Cerretani D, Remondo C, Martellucci I, Marsili S, La Placa M, et al. A novel metronomic chemotherapy regimen of weekly platinum and daily oral etoposide in high-risk non-small cell lung cancer patients. *Oncol Rep.* 2006; 16:133–140. [PubMed: 16786136]
 47. Krzyzanowska MK, Tannock IF, Lockwood G, Knox J, Moore M, Bjarnason GA. A phase II trial of continuous low-dose oral cyclophosphamide and celecoxib in patients with renal cell carcinoma. *Cancer Chemother Pharmacol.* 2007; 60:135–141. [PubMed: 17009033]
 48. Hlushchuk R, Riesterer O, Baum O, Wood J, Gruber G, Pruschy M, et al. Tumor recovery by angiogenic switch from sprouting to intussusceptive angiogenesis after treatment with PTK787/ZK222584 or ionizing radiation. *Am J Pathol.* 2008; 173:1173–1185. [PubMed: 18787105]
 49. Bogunovic D, O'Neill DW, Belitskaya-Levy I, Vacic V, Yu YL, Adams S, et al. Immune profile and mitotic index of metastatic melanoma lesions enhance clinical staging in predicting patient survival. *Proc Natl Acad Sci U S A.* 2009; 106:20429–20434. [PubMed: 19915147]
 50. Baak JP, Gudlaugsson E, Skaland I, Guo LH, Klos J, Lende TH, et al. Proliferation is the strongest prognosticator in node-negative breast cancer: Significance, error sources, alternatives and comparison with molecular prognostic markers. *Breast Cancer Res Treat.* 2009; 115:241–254. [PubMed: 18665447]

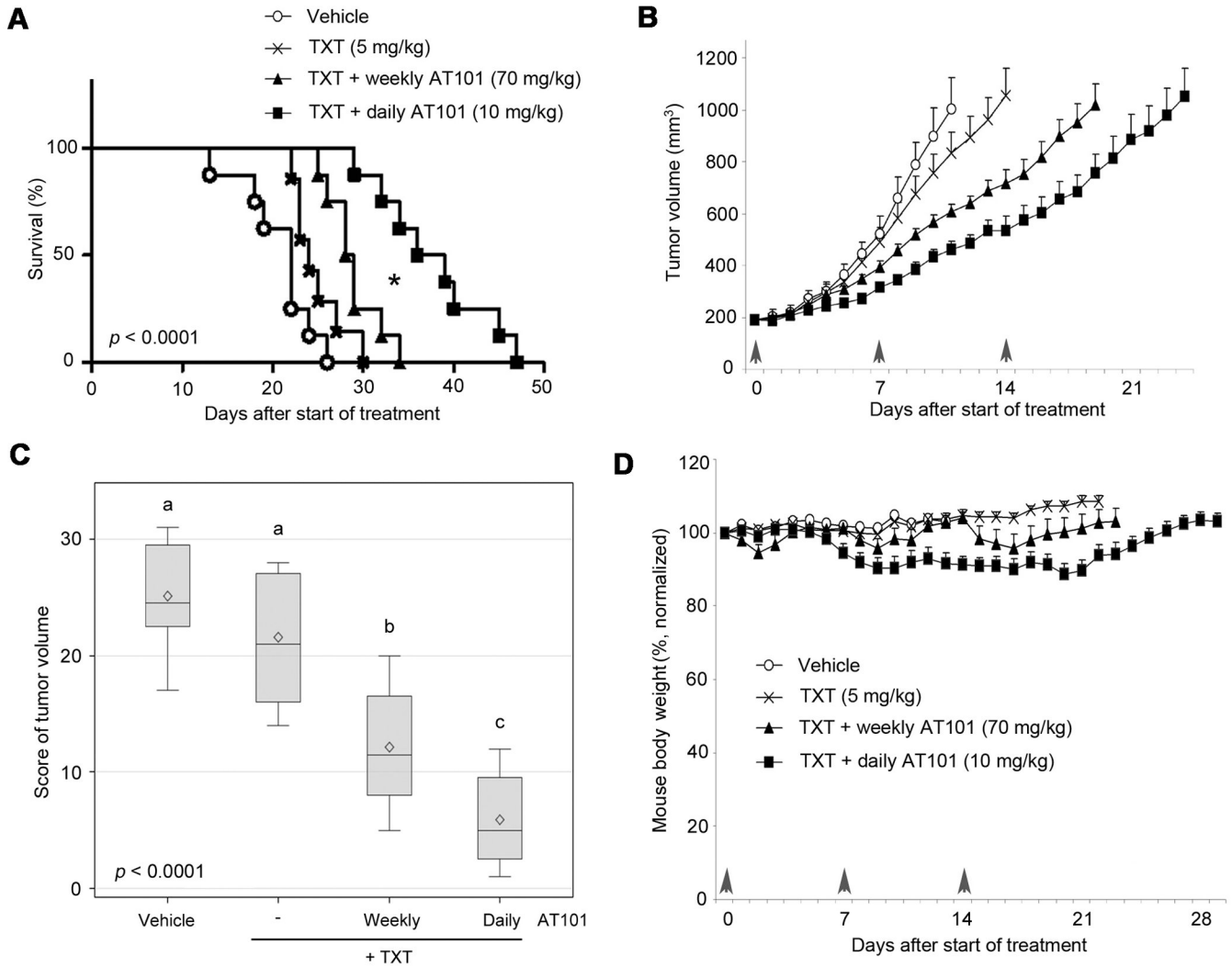


Figure 1. Metronomic AT101 enhances the time to failure of xenograft head and neck tumors. To generate human xenografts vascularized with human vessels, mice received a scaffold seeded with human head and neck squamous cell carcinoma cells (OSCC3) and human endothelial cells. When tumors reached 200 mm³, mice were randomized into the different treatment regimens (vehicle, $n=8$; taxotere, $n=7$; weekly AT101+taxotere, $n=8$; daily AT101+taxotere, $n=8$). Daily administration of low dose AT101 (10 mg/kg) was designated as “metronomic” regimen, while weekly administration of high dose AT101 (70 mg/kg) was designated as “bolus” regimen. In both cases, AT101 was delivered via oral gavage and treatment was performed for 3 weeks. In all conditions, 5 mg/kg taxotere (TXT) were administered weekly via intraperitoneal injection. A, Kaplan-Meier analysis using as criterion for failure a tumor volume of 2,000 mm³. P -value indicates a significant difference across the four groups ($p<0.0001$). Asterisk (*) depicts a statistical difference between weekly AT101+taxotere and daily AT101+taxotere ($p=0.02$). B, graph depicting tumor volume from the first day of treatment through the day when the average tumor volume per group reached 1,000 mm³. C, distribution of Wilcoxon scores for log₂ tumor volume at 13 days of treatment, *i.e.* the day in which the first mouse of the control group had to be euthanized because the tumor reached the cutoff size of 2,000 mm³. P -value indicates a

significant difference across the four groups ($p < 0.0001$). Different letters depict statistically significant differences based on pairwise comparisons ($p < 0.05$). D, graph depicting average body weight during treatment, normalized against pre-treatment weight.

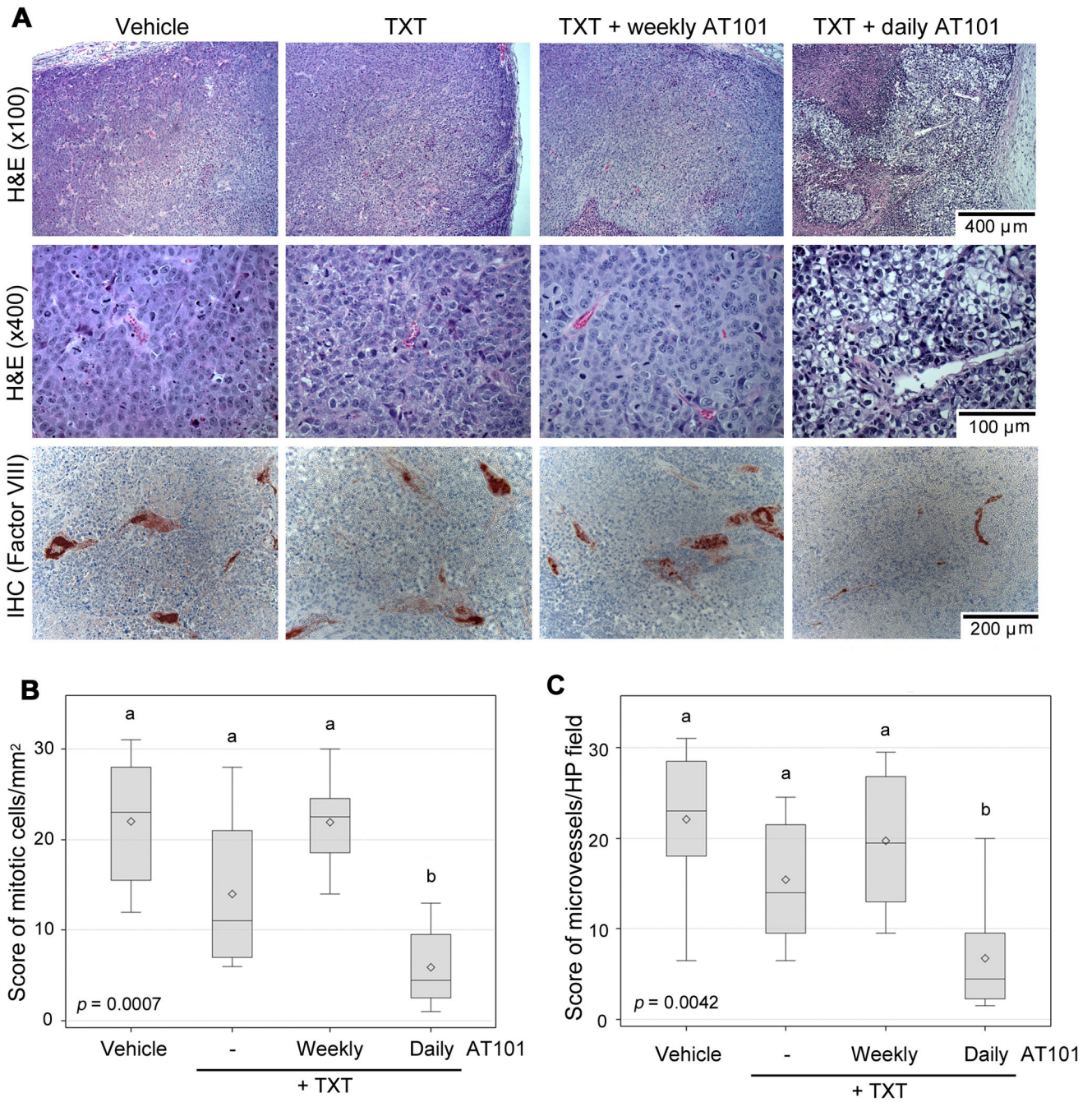
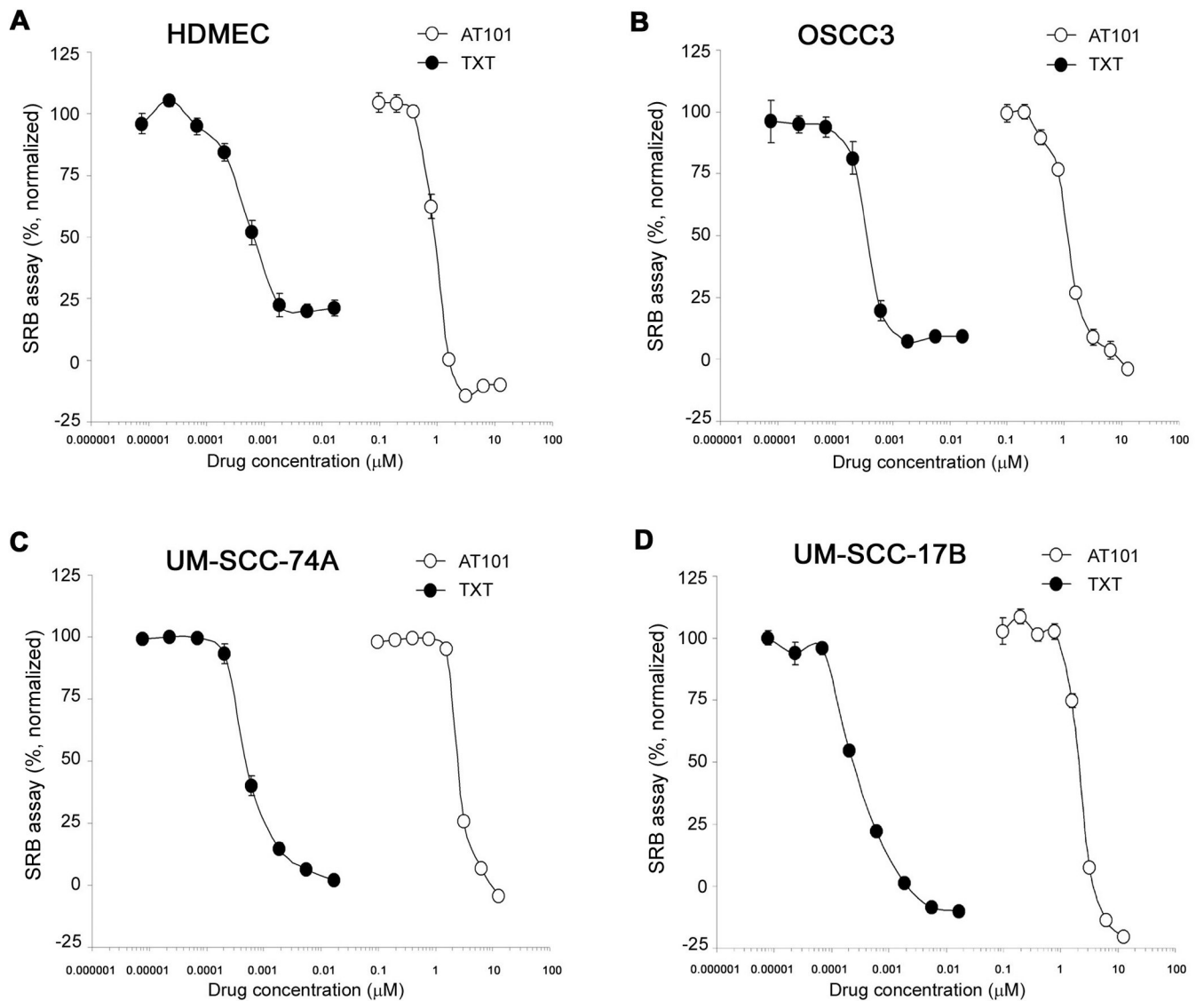


Figure 2. Metronomic AT101 lowers the mitotic index and tumor microvessel density. Paraffin embedded tissue sections were prepared from tumors evaluated in Figure 1. A, representative images of histological sections stained with hematoxylin/eosin (top row, $\times 100$; middle row, $\times 400$). Representative images (bottom row, $\times 200$) of histological sections immunostained for factor VIII (red stain) to identify blood vessels and counterstained with hematoxylin. B, distribution of Wilcoxon scores for average mitotic cells per mm² (mitotic index), as determined by a trained pathologist blinded for experimental conditions. C, distribution of Wilcoxon scores for average tumor microvessel density assessed in 6 high power fields per tumor. *P*-value indicates a significantly difference across the four groups

($p=0.0007$, $p=0.0042$, respectively). Different letters depict statistically significant differences based on pairwise comparisons ($p<0.05$).

**Figure 3.**

Cytotoxic profile of AT101 and taxotere in endothelial cells and head and neck tumor cells. The cytotoxicity was determined by the SRB assay. A to D, cytotoxicity of AT101 and taxotere (TXT) on human dermal microvascular endothelial cells (HDMEC) and head and neck squamous cell carcinoma cells (OSCC3, UM-SCC-74A, UM-SCC-17B). Cells were exposed to AT101 or TXT for 72 hours. Data were normalized against vehicle control and initial plating density. Experiments were done in triplicate wells per condition. Each graph is representative of three independent experiments.

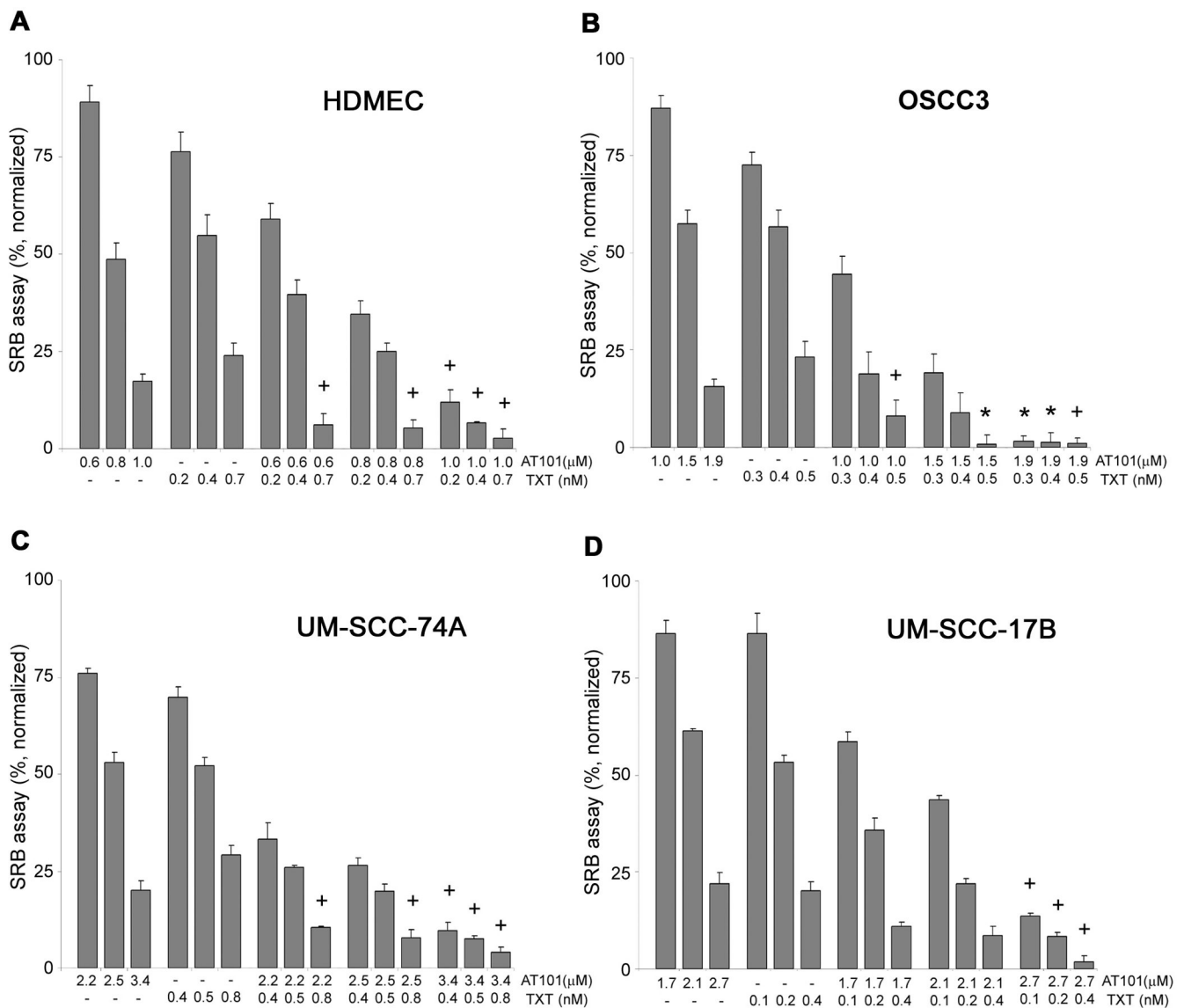


Figure 4. Effect of AT101 and taxotere drug combination on endothelial cells and head and neck tumor cells. The cytotoxicity was determined by the SRB assay. A to D, cells were exposed to AT101 or taxotere (TXT) for 72 hours. The concentrations selected for this study were the IC₂₅, IC₅₀ and IC₇₅ for each drug in each cell line. Combinatorial Index (CI) was calculated for each experimental condition. Asterisk (*) depicts synergistic effect (CI<0.9), while a plus sign (+) depicts additive effect (0.9 < CI < 1.1). Data were normalized against vehicle control and initial plating density. Experiments were done in triplicate wells per condition. Each graph is representative of three independent experiments.

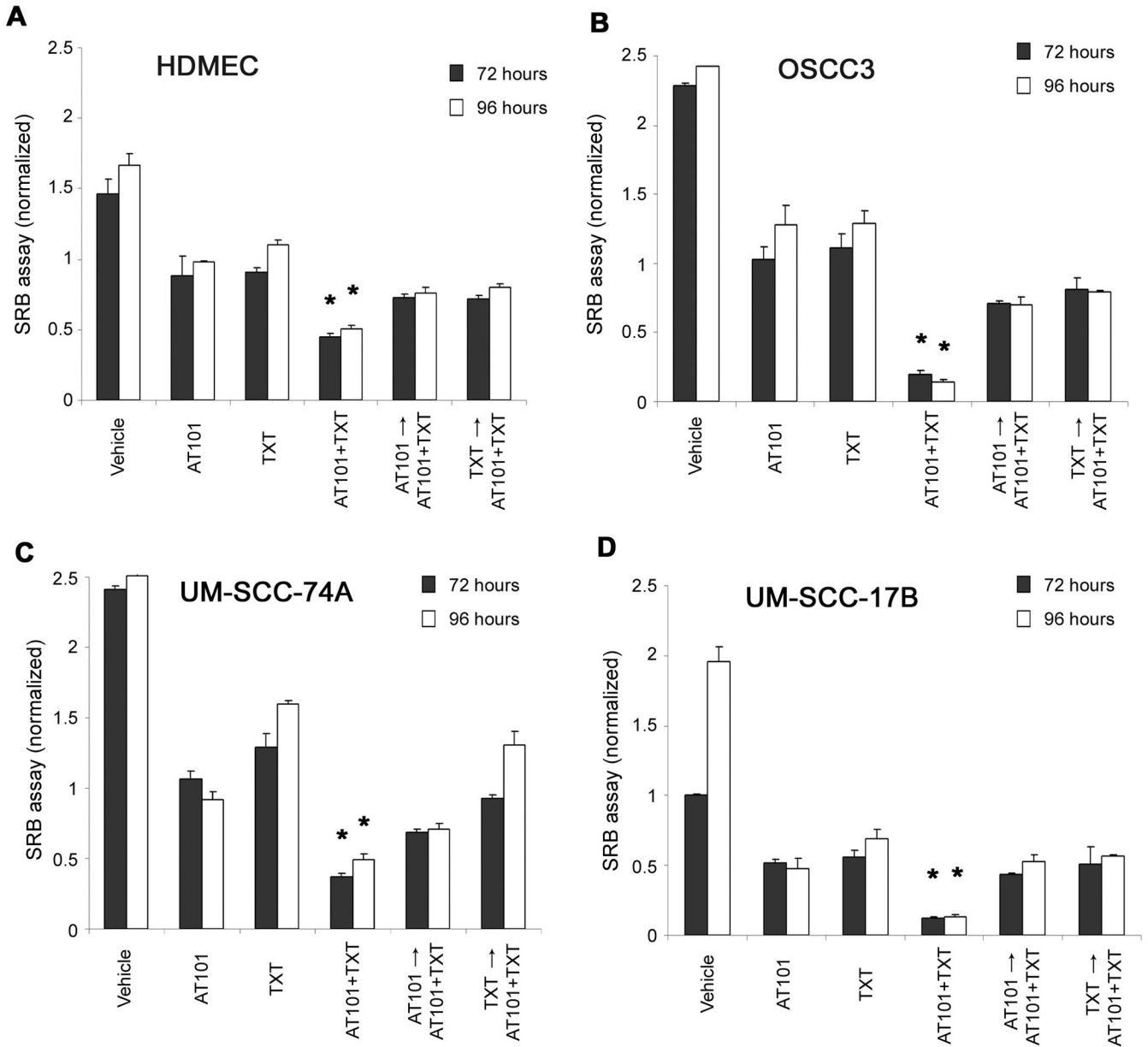


Figure 5. Effect of drug sequence on endothelial cells and head and neck tumor cells. A to D, cells were exposed to the IC₅₀ concentration of each drug, and cytotoxicity was determined by the SRB assay. Cells were pre-treated either with AT101 or with TXT for 24 hours. Then, cells were exposed to AT101 or taxotere (TXT) for additional 48 or 72 hours. Alternatively, treatment was performed with both drugs administered at the same time, or performed with single-drug as controls. Asterisk (*) depicts statistically significant differences at $p < 0.01$. Data were normalized against initial plating density. Experiments were done in triplicate wells per condition. Each graph is representative of three independent experiments.

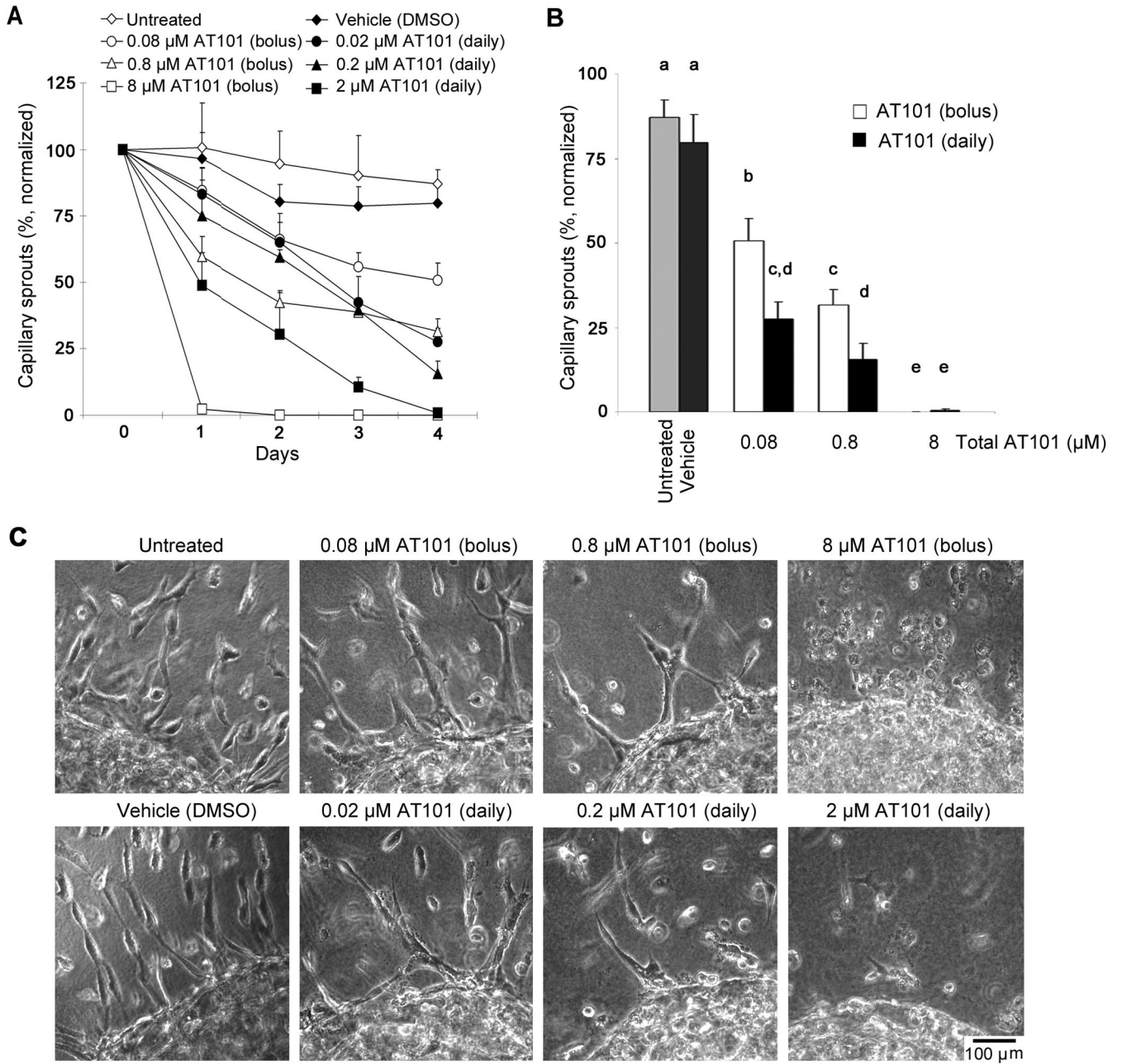


Figure 6. Effect of metronomic versus bolus AT101 on the angiogenic potential of human endothelial cells. The effect of AT101 on the angiogenic potential was evaluated in primary human dermal microvascular endothelial cells (HDMEC) plated in 3-D collagen matrices. A, graph depicting the number of capillary sprouts in VEGF-treated HDMEC exposed to AT101 for 4 days. AT101 was used at the following concentrations: $0.1 \times IC_{50}$ (0.08 μ M), IC_{50} (0.8 μ M), $10 \times IC_{50}$ (8 μ M). In the metronomic group, $1/4$ of the IC_{50} was administered daily (from day 0 to 3); while in the bolus treatment group, the full dose was administered on day 0. The total amount of drug was the same in the metronomic and bolus treatment group. B, graph depicting the number of sprouts at the end of the experimental period. Different letters depict statistically significant differences at $p < 0.05$. C, representative photomicrographs of

capillary sprouts ($\times 150$) at the end of the experimental period. Results were normalized against initial number of sprouts. Experiments were done in triplicate wells per condition. Data is representative of three independent experiments.